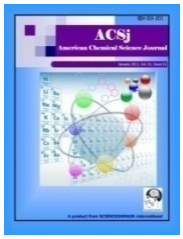

*American Chemical Science Journal*
*4(6): 745-758, 2014*

**SCIENCEDOMAIN** *international*
www.sciencedomain.org

# Investigation of New Ionic Plastic Crystals in $NR_4BBu_4$ (R = Me, Et, Pr, Bu, Pen)

**Tomoyuki Hayasaki[1], Satoru Hirakawa[1]and Hisashi Honda[1*]**

*[1]Graduate School of Nanobioscience, Yokohama City University, Kanazawa-ku, Yokohama, 236-0027, Japan.*

***Authors' contributions***

*This work was carried out in collaboration between all authors. All authors contributed in practical work and managed the analysis of the study. All authors read and approved the final manuscript.*

***Original Research Article***

***Received 24th March 2014***
***Accepted 22nd April 2014***
***Published 24th May2014***

## ABSTRACT

In order to investigate new ionic plastic crystals, differential-scanning-calorimetry (DSC), nuclear-magnetic-resonance (NMR), and electrical conductivity measurements were carried out in $NR_4BBu_4$ (R = Me, Et, Pr, Bu, Pen) salts. DSC measurements showed a low entropy change of 29.1 J $K^{-1}$ $mol^{-1}$ at a melting point and large values of 35.7 and 17.8J $K^{-1}$ $mol^{-1}$ at phase transitions in $NEt_4BBu_4$ crystals. In contrast, the other compounds of $NR_4BBu_4$ (R = Me, Pr, Bu, Pen) showed large entropy changes at each melting point. On the basis of solid-state $^1H$ and $^{13}C$ NMR spectra results, tumbling motions were detected in the $NMe_4BBu_4$ and $NEt_4BBu_4$ crystals. Isotropic reorientation motions of partial ions were observed in the $NPr_4BBu_4$ crystals. Although $NR_4BBu_4$ (R = Me, Et, Pr) have no plastic phases, low activation energies of ion transfer were recorded in these salts. These results suggest that the tumbling motions can perform the resemble effect as isotropic reorientation in plastic crystals.

*Keywords: Plastic crystal; Ionic conductor; isotropic reorientation; tumbling motion.*

## 1. INTRODUCTION

Plastic crystals are soft materials in solids. The constituents are isotropically rotated at each crystal-lattice point, i.e.the particle has fused orientation (liquid character)and the gravity

**Corresponding author: Email: hhonda@yokohama-cu.ac.jp;*

point of each constituent is ordered (crystal character). Therefore, they belong to an intermediate phase between solid and liquid; materials of inverse character are called liquid crystal. On disordering a particle's orientation in plastic crystals, small entropy changes at each melting point ($\Delta S_{mp}$< 20 J $K^{-1}$ $mol^{-1}$) and a large $\Delta S_{tr}$ value at a transition temperature between solid phases can be detected [1]. In addition, self-diffusion of constituent particles is observed in plastic phases. This translation causes plasticity in solid substances. Plastic crystal can be classified as either ionic or molecular based upon its constituent particles. In molecular plastic crystals, globular molecules e.g. fullerene, adamantane, tetrachloromethane, etc., have plastic phases [2-9]. The globular molecular shapes and weak intermolecular attractions are key points for isotropic reorientation and self-diffusion of molecules with low activation energies. In contrast, ionic plastic crystals are formed by a globular ion and a non-globular counter ion with formulas $MNO_2$ (M = K, Rb, Cs, Tl, and $NH_4$) [10-24], $[C_5H_{10}N(CH_3)_2]SCN$ [25],$N(CH_3)_4N_3$ [26], piperidinium X (X = $ClO_4$, $PF_6$, $NO_3$) [27,28],etc. Based on NMR studies of $MNO_2$, a revolving door model has been proposed for ionic translation [23,29]. In this model, isotropic reorientation rates of the plane anion (the revolving gate) are slow enough for the cation (the human) to diffuse through the plane formed by the anions. From the translating cation's point of view, the anions appear frozen. That is, the translation model is the difference between molecular and ionic plastic crystals. The difference is caused by constituents' shapes and strengths of interactions acting on particles. Based on this fact, we have proposeda new type of ionic plastic crystal [30] in which a globular cation and anion perform isotropic reorientation if the Coulomb force among the ions is weak enough. In the new region of plastic crystal, we have succeeded in showing the new type of ionic plastic crystals as reported for $NR_4BEt_3Me$ (R = Me, Et) and $NEt_xR'_{4-x}BEt_3Me$ (R' = Me, Pr. $x$ = 1-3) [30].Differential-scanning-calorimetry (DSC) measurements of these $BEt_3Me$ salts show small $\Delta S_{mp}$ and large $\Delta S_{tr}$ values at phase-transition temperatures in the plastic phase. In addition, these crystals can be transformed to the plastic phase with low temperatures and have high melting points. The former result is frequently detected in molecular plastic crystals while the latter is often found in ionic plastic crystals.$^1$H and $^{13}$C NMR spectra of these $BEt_3Me$ compounds additionally reveal isotropic reorientation motion in the plastic phase. Ionic conductivity measurements also show self-diffusion of both ions with low activation energies. Based on these results, the new region of ionic plastic crystal shows characteristics of ionic and molecular plastic crystals.

In this study, we treated crystals containing a $BBu_4^-$ anion in exchanging of a $BEt_3Me^-$ ion: $NR_4BBu_4$ (R = Me, Et, Pr, Bu, Pen) was prepared. In order to compare with results reported in $BEt_3Me$ salts [30], DSC, NMR, and ionic conductivity measurements were performed.

## 2. EXPERIMENTALS

### 2.1 Sample Preparation

Crystals of $NR_4BBu_4$ (R = Me, Et, Pr, Bu, Pen) were prepared by adding $LiBBu_4$ into $NR_4Br$ in aqueous solution. Certain compounds of $NR_4Br$ were obtained commercially: $NMe_4Br$ (Wako Junyaku Co.); $NEt_4Br$ and $NPr_4Br$ (Kanto Kagaku Co.);and $NBu_4Br$ and $NPen_4I$ (Tokyo Kasei Industry Co.). For preparation of $LiBBu_4$, the previously reported recipe [31] was slightly altered. A three-necked flask equipped with a stirrer, silicon caps, condenser, and thermometer was used. Air in the flask was substituted by dried $N_2$ gas. 30 $cm^3$ of diethyl ether dried by molecular sieves was placed in the flask. After keeping the liquid temperature at 0ºC, 45.5 $cm^3$ of *n*-BuLi in *n*-hexane diluent (1.65 mol $dm^{-3}$) (Kanto Kagaku Co.)was added into the flask. 2 $cm^3$ of $BF_3$ in diethyl ether solution (0.016 mol) was slowly added into the

flask at 0°C with continuous stirring for 3 h. After stirring the solution at room temperature for 12 h, the solution was cooled at 0°C again, and in order to decompose the unreacted *n*-BuLi, a small amount of ethanol was gradually poured into the flask until a colorless solution was obtained. After evaporating diethyl ether and hexane until the solution showed viscosity, each $NR_4$ salt (0.021 mol) in aqueous solution of 300 $cm^3$ was added. After stirring the solution for 1 h and filtering, crude samples containing $NR_4BBu_4$wereobtained. The crude samples were recrystallized from a mixed solution of acetone(10 $cm^3$) and water(400 $cm^3$) in a desiccator with $P_2O_5$as the drying agent for 1 day; air in the desiccator was substituted by dried $N_2$ gas.

## 2.2 Measurements

Because the specimens were hygroscopic, the following manipulations were carried out under a dry $N_2$ gas atmosphere.

DSC spectra were obtained with a Shimadzu DSC-60 and Seiko Instruments Inc. SSC/5200 calorimeter with a reference sample of $Al_2O_3$. The samples were heated from ca. 210 K at rates of 5 K $min^{-1}$. From these results, melting points ($T_{mp}$) and transition temperatures in the solid phase were determined, as well as entropy changes at these transition temperatures.

Electrical conductivity measurements were performed at 1 kHz with a two-terminal method employing an Andou AG-4303 LCR meter equipped with an Al sheet. The powdered sample was pressed into a disc of 1 cm in diameter and ca. 1mm thick. For measurements, the air around the probe was replaced by dry $N_2$ gas.

Solid-state $^1$H NMR spectra were recorded at a Larmor frequency of 600.13 MHz using a Bruker Avance 600 spectrometer (14.01 T). The samples were packed in a $ZrO_2$ rotor with an outer diameter of 4.0 mm. A magic-angle-spinning (MAS) method with 10 kHz was used. $^1$H NMR spectra were obtained by Fourier transformation (FT) of free-induction-decay (FID) signals that were obtained after a $\pi/2$ pulse. $^1$H chemical shifts (CS) were calibrated relative to an external adamantane ($\delta$ = 1.91 ppm) reference. Spin-lattice relaxation time ($T_1$) of the$^1$H nucleus was estimated using an inversion recovery method ($\pi_x$ - $t$ - $(\pi/2)_x$ - FID). In these measurements, a recycle time of 5 s was employed. Sample temperature was controlled and recorded with a Bruker VT-2000. Solid-state $^{13}$C NMR spectra were observed at a Larmor frequency of 150.92 MHz using the same spectrometer. The same sample tubes asthose of the $^1$H measurements were employed. $^{13}$C NMR spectra were obtained with a $^1$H decoupling pulse sequence. CS of the $^{13}$C nuclei were calibrated with an external adamantane ($\delta$ = 29.47 ppm) reference. $^{13}$C MAS NMR spectra were plotted with MAS ratios of 1 and 5 kHz. Static $^{13}$C NMR measurements were also carried out. In both observations, a recycle time of 20 s was used. A cross-polarization (CP) method was also employed to detect motional modulationin the Hartmann–Hahn condition. Contact times of 0.5, 1.0, and 2.0 ms were introduced. Recycle times of 5 and 10s were used for$^{13}$C CP/MAS NMR and static$^{13}$C CP NMR measurements, respectively. In order to check purity of synthesized specimens, $^1$H and $^{13}$C NMR measurements of the prepared sample dissolved in DMSO-*d*6 solvent were performed with the same spectrometer; this apparatus can measure solution and solid samples by exchanging the probe. Glass tubes of 5.0 mm in a diameter were used for solution measurements. CS values of $^1$H and $^{13}$C nucleus were calibrated with an inner reference of tetramethylsilane (TMS) ($\delta$ = 0.00 ppm). $^1$H and $^{13}$C NMR measurements in DMSO solution showed that whole products treated in the present study were successfully prepared with high purity.

## 3. RESULTS AND DISCUSSION

### 3.1 DSC Results

DSC thermograms observed in $NR_4BBu_4$ (R = Me, Et, Pr, Bu, Pen) crystals are shown in Fig. 1. The variation appearing at the initial temperature range (whole measurements were started at the low temperature) is due to instrument noise. In this paper, the symbols $T_{mp}$ and $T_{tr1}$, $T_{tr2}$, etc., are employed to indicate the phase-transition temperatures at the melting point and in solid phases moving from higher to lower temperatures; and Phase I, Phase II, etc., are used to designate the solid phases from the highest-temperature solid-phase of each crystal. The values of $T_{mp}$ and $T_{tr1}$, $T_{tr2}$, etc., and the entropy changesat the melting point ($\Delta S_{mp}$) and at each transition temperature ($\Delta S_{tr1}$, $\Delta S_{tr2}$, etc.)obtained in each salt are listed in Table 1.

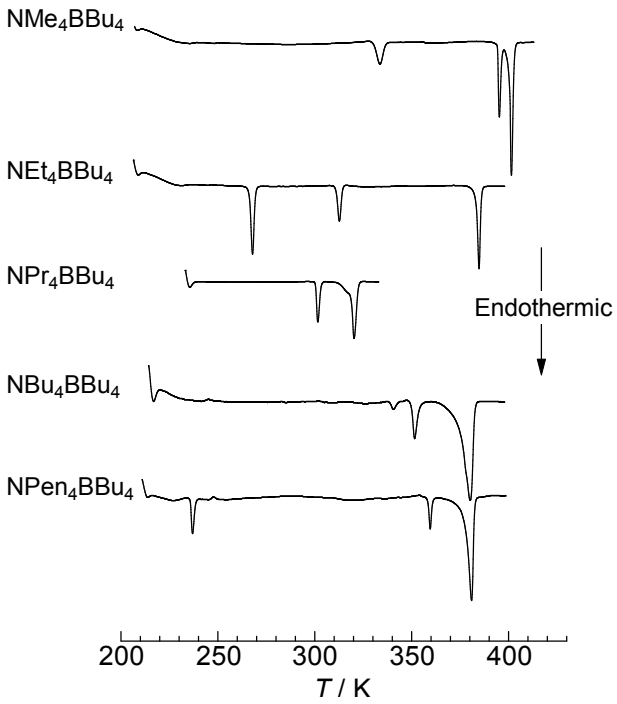


**Fig. 1. DSC thermograms of $NMe_4BBu_4$, $NEt_4BBu_4$, $NPr_4BBu_4$, $NBu_4BBu_4$, and $NPen_4BBu_4$**

**Table 1. Entropy changes ($\Delta S$) in J $mol^{-1}$ $K^{-1}$ at each phase transition temperature and melting point in $N(n\text{-}C_xH_{(2x+1)})_4B(n\text{-}C_4H_9)_4$ ($x$ = 1-5) salts. Each temperature is displayed in parenthesis (unit is K)**

| | $\Delta S_{tr2}$ ($T_{tr2}$) | $\Delta S_{tr1}$ ($T_{tr1}$) | $\Delta S_{mp}$ ($T_{mp}$) |
|---|---|---|---|
| $NMe_4BBu_4$ | 14.2 (330.2) | 13.1 (393.8) | 58.4 (401.7) |
| $NEt_4BBu_4$ | 35.7 (266.0) | 17.8 (310.6) | 29.1 (383.0) |
| $NPr_4BBu_4$ | | 22.3 (304.9) | 52.5 (322.7) |
| $NBu_4BBu_4$ | 2.6 (338.1) | 10.5 (357.9) | 56.2 (373.6) |
| $NPen_4BBu_4$ | 16.6 (235.7) | 9.0 (354.5) | 68.2 (376.7) |

The smallest $\Delta S_{mp}$ value of 29.1 J $K^{-1}$ $mol^{-1}$was obtained in the $NEt_4BBu_4$ crystal. This value was unsatisfied to the condition of plastic crystal (< 20 J $K^{-1}$ $mol^{-1}$ [1]), however, the total amount of entropy change in solid phases ($\Delta S_{tr1}$ + $\Delta S_{tr2}$) was larger than $\Delta S_{mp}$. This fact suggests that ionic motions with a large degree of freedom exist in the solid phases. In contrast, large $\Delta S_{mp}$ values and small entropy changes in solid phases were obtained in the other $NR_4BBu_4$-type salts.

## 3.2 DFT Simulations

In order to obtain information about ionic motions for each salt, solid-state NMR measurements were carried out. In addition, density-functional-theory (DFT) simulation was performed to assign NMR peaks and to estimate line-widths observed on $^1$H and $^{13}$C NMR spectra. As it has been demonstrated in the previous report [30] that a B3LYP/6-311+G** function can explain the $^{13}$C NMR CS values and line-widths observed in alkylammoniumions and a $BEt_3Me^-$ion well, the same procedure was used in this study. Whole atomic coordinates in each cation and a $BBu_4^-$ion were optimized by the B3LYP/6-311+G** function in the Gaussian 03 computer program [32] before calculating shieldingtensors. CS values were obtained by subtracting the isotropic value of the shielding tensors estimated in the cation and anion from that of a tetramethylsilane (TMS) molecule, where an isotropic shieldingtensor of TMS was simulated by the same process as described above. The$^{13}$C NMR line-widths were estimated by anisotropic shieldingtensors. $^1$H and $^{13}$C CS values and $^{13}$C NMR line-widths obtained by this computer simulation are summarized in Table 2.

**Table 2. Chemical shift (CS) values of $^1$H and $^{13}$C NMR signals and line widths of $^{13}$C nucleus simulated by B3LYP/6-311+G**. Values are given in ppm**

| **$^1$H CS values** | | | | | |
|---|---|---|---|---|---|
| **Ions** | α | β | γ | δ | ε |
| $NMe_4^+$ | 3.10 | | | | |
| $NEt_4^+$ | 3.16 | 1.50 | | | |
| $NPr_4^+$ | 2.93 | 1.70 | 1.18 | | |
| $NBu_4^+$ | 2.96 | 1.59 | 1.37 | 1.26 | |
| $NPen_4^+$ | 3.02 | 1.70 | 1.20 | 1.49 | 0.92 |
| $BBu_4^-$ | 0.18 | 1.24 | 1.18 | 0.86 | |
| **$^{13}$C CS Values** | | | | | |
| **Ions** | α | β | γ | δ | ε |
| $NMe_4^+$ | 58.26 | | | | |
| $NEt_4^+$ | 63.03 | 11.44 | | | |
| $NPr_4^+$ | 70.35 | 21.85 | 15.49 | | |
| $NBu_4^+$ | 69.22 | 30.95 | 25.56 | 15.89 | |
| $NPen_4^+$ | 72.08 | 31.44 | 34.61 | 28.79 | 15.23 |
| $BBu_4^-$ | 37.41 | 37.81 | 36.92 | 15.89 | |
| **$^{13}$C CS Line-Widths** | | | | | |
| **Ions** | α | β | γ | δ | ε |
| $NMe_4^+$ | 85.40 | | | | |
| $NEt_4^+$ | 85.40 | 21.91 | | | |
| $NPr_4^+$ | 90.54 | 21.94 | 26.46 | | |
| $NBu_4^+$ | 88.53 | 37.96 | 26.13 | 30.21 | |
| $NPen_4^+$ | 69.98 | 29.93 | 34.65 | 23.26 | 29.26 |
| $BBu_4^-$ | 37.22 | 41.00 | 40.13 | 34.13 | |

DFT simulation also gave ionic radius: $NMe_4^+$ (210), $NEt_4^+$ (320), $NPr_4^+$ (440), $NBu_4^+$ (560), $NPen_4^+$ (670), and $BBu_4^-$ (590 pm). Since ionsize ratios (cation/anion) of NaCl and CsCl are 0.535 and 0.939, respectively, it can be expected that $NEt_4BBu_4$ (ratio of 0.54), $NPr_4BBu_4$ (0.74), and $NBu_4BBu_4$ (0.94) have a cubic structure if both cation and anion can perform isotropic reorientations.

## 3.3 NMR Results

### 3.3.1 $NEt_4BBu_4$

$^1$H MAS NMR spectra obtained in $NEt_4BBu_4$ are shown in Fig. 2(a). Intensities of the signals recorded at -0.02, 0.96, and 1.30 ppm were increased with temperature in Phase I. Our CS simulation indicates that these signals were assignable to H atoms of $BC\underline{H}_2C_3H_7$, $BC_3H_6C\underline{H}_3$, and $BCH_2C_2\underline{H}_4CH_3$ in the anion, respectively. This figure suggests that anion motions reduce dipole-dipole interaction among H atoms in Phase I, although strong $^1$H-$^1$H linkage is retained in Phase II. The other signals recorded at 1.48 and 3.42 ppm were assignable to the H atoms of $C\underline{H}_3$ and $C\underline{H}_2$ in the $NEt_4^+$ ion, respectively. The narrow line-width of these cation peaks were almost independent of temperature. Based on these results, it can be considered that the cation has overall motions with large amplitudes in Phase I and II. In the case of $^{13}$C MAS NMR spectra, three sharp peaks at 10.2, 17.3, and 56.1 ppm, and two weak signals at 31.2 and 33.1 ppm were observed at 350 K as shown in Fig. 2(b). Based on our CS calculation, the peaks observed at 10.2 and 56.1 ppm were attributable to $\underline{C}H_3$ and $\underline{C}H_2$ in the $NEt_4^+$ ion, respectively. These two signals preserve the line-widths and intensities with temperature, leading to the view that the cation undergoes motions with large amplitudes in the solid phases. This result is consistent with those of $^1$H MAS NMR lines. Each $^{13}$C MAS NMR line was accompanied with a few spinning-side-band (SSB) signals at 350 K. Since the line-widths of 0.2 ($NCH_2\underline{C}H_3$), 13.2 ($N\underline{C}H_2CH_3$), 13.2 ($BC_3H_6\underline{C}H_3$), and 13.2 ($BCH_2\underline{C}_2H_4CH_3$), and 13.2 ($B\underline{C}H_2C_3H_7$) ppm estimated by SSB signals are smaller than the simulated values of 21.9, 85.4, 34.1, 40.5, and 37.2 ppm, respectively, it can be considered that both ions' motions average chemical-shift-anisotropy (CSA) at each C atom in Phase I. However, these line-breadths suggest that no isotropic reorientation occurs for either ion. Based on these NMR results, an acceptable model of overall motion is a tumbling ion, which is consistent with results of DSC measurements showing large ($\Delta S_{tr1}$ + $\Delta S_{tr2}$) and small $\Delta S_{mp}$ values. $^{13}$C CP/MAS NMR measurements were carried out as a function of contact times ($\tau_c$). The results obtained at 320 K are shown in Fig. 2(c). In general, the CP method enhances signal intensities of sparse spin in crystals. However, if $^1$H nuclei have short spin-lattice relaxation times in rotating frame ($T_{1\rho}$) or there is isotropic reorientation motion, the signal intensities on CP spectra are conversely reduced [33]. In Fig. 2(c), the intensities of the anion's peaks recorded at 17.3, 31.2, and 33.1 ppm became small with increasing $\tau_c$, although the signal intensities observed at 10.2 and 56.1 ppm were independent with $\tau_c$. Based on the fact that $^{13}$C MAS NMR spectra negate isotropic reorientation motions, it can be considered that this reducing intensity is caused by short $T_{1\rho}$ values. In order to reveal motional modes, $^1$H $T_1$ measurements were performed with an inversion recovery method. Obtained $^1$H NMR $T_1$ values are displayed in Fig. 2(d). The $T_1$ values of the cation and anion increased monotonously with temperature. Because the $^1$H $T_1$ process can be attributed to $^1$H-$^1$H dipole-dipole interactions, it is considered that there is a fast motion compared to the observed frequency of 600.13 MHz. In contrast, $^1$H $T_{1\rho}$ values were estimated to be on the order of a few ms by $^{13}$C CP/MAS NMR measurements. Therefore, it can be concluded that different motions are attributed to the $T_1$ and $T_{1\rho}$ processes. Based on the positive $T_1$ slope, it can be expected that the tumbling motion reducing $^1$H line-widths effects onto the $T_1$ process

and ion transfer contributes to $T_{1\rho}$. Applying the following relation [34] to the observed $T_1$ values, an activation energy ($E_a$) can be estimated for each ion in the $NEt_4BBu_4$ crystal.

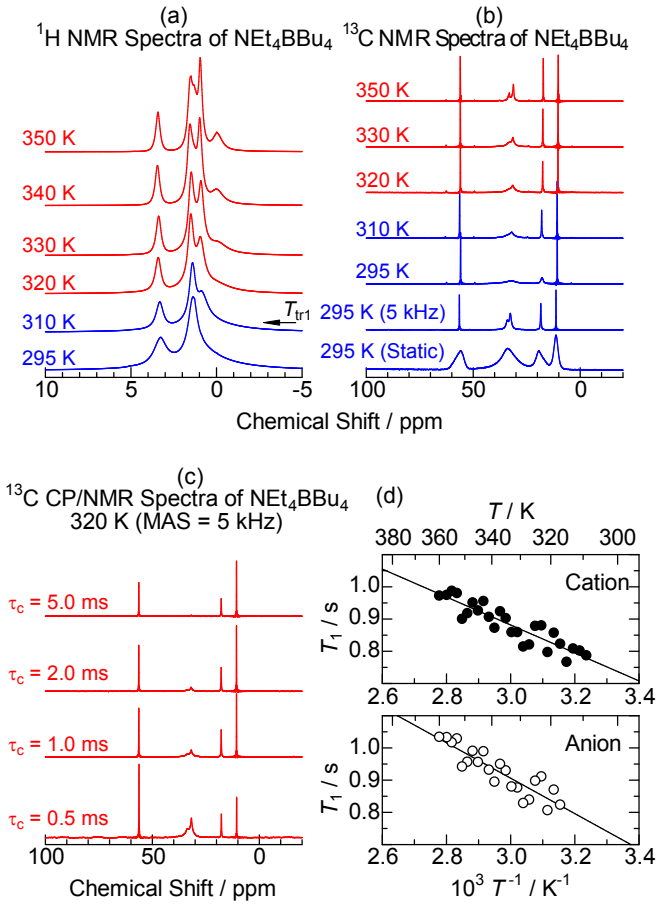


**Fig. 2. $^1$H MAS and $^{13}$C NMR spectra and spin-lattice relaxation times ($T_1$) of $NEt_4BBu_4$. In this figure, spectra recorded in Phase I and II are shown by red and blue lines, respectively. (a) $^1$H MAS NMR lines observed at a MAS ratio of 10 kHz. (b) $^{13}$C MAS NMR spectra recorded at 1 kHz except for two lines (rates are described in parenthesis). (c) Contact time ($\tau_c$) dependences of $^{13}$C CP/MAS NMR spectra observed with MAS = 5 kHz at 320 K. (d) $T_1$ values obtained by an inversion recovery method**

$$\frac{1}{T_1} = C\tau\left[\tau = \tau_0 \exp\left(\frac{E_a}{RT}\right)\right] \quad (1)$$

Here, $C$, $\tau$, and $\tau_0$ are a proportional constant relating to the character of motion, and correlation time at a certain temperature and infinite temperature, respectively. The similar $E_a$ values of 5±1 and 6±1 kJ $mol^{-1}$ were estimated for $NEt_4^+$ and $BBu_4^-$ ions, respectively. These values are analogous to those of isotropic reorientation reported in ordinal ionic-plastic-crystals [2-15, 25].

### 3.3.2 $NMe_4BBu_4$

The results of $^1H$ MAS NMR spectra obtained in $NMe_4BBu_4$ are shown in Fig. 3(a). A large intensity signal of $^1H$ MAS NMR was recorded at 2.98 ppm. Based on our CS simulation, this signal can be attributed to the H atoms of the $NMe_4^+$ ion. In contrast to this broad signal, two weak peaks were recorded at 0.59 and 1.01 ppm on the $^1H$ MAS NMR spectra in Phase III. After $T_{tr2}$, the former peak was recorded at 0.42 ppm and two new peaks were observed at 0.21 and 0.64 ppm, in addition, another broad signal with line-width of ca. 2.5 ppm was observed at ca. 0.6 ppm. As these signals of 0.21 and 0.64 ppm (sharp) and 0.6 ppm (broad) were recorded in the same CS range as the anion's H signals, it is thought that there are some states of alkyl chains in the anion: Certain alkyl chains have motions reducing $^1H$-$^1H$ dipole-dipole interactions, and the others are restricted to the crystal. In the case of $^{13}C$ MAS NMR spectra, three strong signals were recorded at 14.9, 29.1, and 55.4 ppm with MAS = 5 kHz in Phase III as displayed in Fig. 3(b). Based on the result of our CS simulation, signals at 14.9 and 29.1 ppm can be assigned to $BC_3H_6\underline{C}H_3$ and $B\underline{C}_3H_6CH_3$, respectively. The line-widths of 19.8 ($\underline{C}H_3$ of $BBu_4^-$) and 39.6 ($\underline{C}H_2$ of $BBu_4^-$) ppm were estimated from SSB signals. The later was similar to simulated values of 37.2 ($\alpha$-$CH_2$), 41.0 ($\beta$-$CH_2$), and 40.1 ppm ($\gamma$-$CH_2$) in the $BBu_4^-$ ion,conversely, the former value of 19.8 ppm was smaller than 34.1 ppm ($\underline{C}H_3$). Based on these results, it can be considered that there are motions of $CH_3$ rotation about $CH_2$-$CH_3$ of the $BBu_4^-$ ion in Phase III. In the case of the cation's signal, a line-width of 6.6 ppm was observed at 55.4 ppm. This width is much smaller than the simulated value of 85.40 ppm. In addition, the Lorentz-like line-shape was recorded on the $^{13}C$ static spectrum. These results suggest that CSA of the $^{13}C$ nucleus in the $NMe_4^+$ ion was averaged at around room temperatures. To satisfy this result, we can construct a model of overall motion (tumbling). On the $^1H$ MAS NMR spectra, cation signals show a large line-width of 1.3 ppm. This result indicates that dipole-dipole interactions among the H atoms remain due to overall motion. Based on these $^1H$ and $^{13}C$ NMR results, it can be considered that the cation has a slow overall motion in a site enclosed by alkyl chains of the anions (the cation penetrates into the anion). This model can also explain the result that the $CH_2$group of the anions are restricted to the crystal and only the $CH_3$ group can be rotated.

### 3.3.3 $NPr_4BBu_4$

$^1H$ and $^{13}C$ NMR spectra observed in $NPr_4BBu_4$ are displayed in Fig. 4. Six signals with narrow line-width and an additional peak with a broad breadth at 1.1 ppm were recorded on the $^1H$ MAS NMR spectra in Phase I and II. In the case of $^{13}C$ MAS NMR spectra observed at 295 K with MAS = 5 kHz, two sharp peaks and one envelope imposed by a few signals, and one broad line with low intensity were recorded at 18.3 and 23.0 ppm and at 37 ppm, and at 68 ppm, respectively. SSB signals of the $^{13}C$ MAS spectra detected at 295 K were reduced after the $T_{tr1}$ transition, however tails were recorded on each peak. This result indicates that there are at least two kinds of ions in the crystal: One shows sharp signals and the others give broad lines. This model can also explain the $^1H$ MAS NMR spectra. The $^{13}C$ CP/MAS NMR signals showed similar line-widths to those of the tail components observed on the $^{13}C$ MAS spectrum, therefore, it can be considered that some ions perform isotropic reorientation and the others are rigid in the crystal.

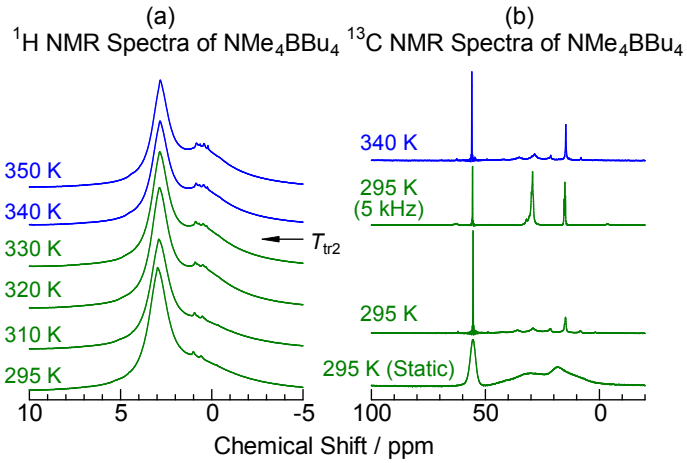


**Fig. 3. $^{1}$H MAS and $^{13}$C NMR spectra of $NMe_4BBu_4$ as a function of temperature.In this figure, spectra recorded in Phase II and III are shown by blue and green lines, respectively. (a) $^{1}$H MAS NMR lines observed at a MAS ratio of 10 kHz. (b) $^{13}$C MAS NMR spectra measurements performed at MAS = 1 kHz except for two lines (rates are described in parenthesis)**

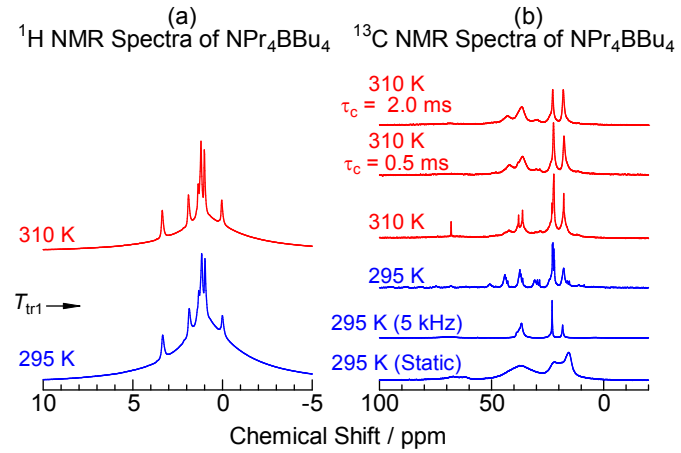


**Fig. 4. $^{1}$H MAS and $^{13}$C NMR spectra of $NPr_4BBu_4$ as a function of temperature. In this figure, spectra recorded in Phase I and II are shown by red and blue lines, respectively. (a) $^{1}$H MAS NMR lines observed at a MAS ratio of 10 kHz. (b) $^{13}$C MAS NMR spectra recorded at MAS = 1 kHz except for two lines (rates are described in parenthesis). Contact times ($\tau_c$) are described on $^{13}$C CP/MAS NMR spectra**

### 3.3.4 $NBu_4BBu_4$ and $NPen_4BBu_4$

$^{1}$H and $^{13}$C MAS NMR spectra observed in $NBu_4BBu_4$ and $NPen_4BBu_4$ crystals are shown in Fig. 5. Since the $^{13}$C MAS NMR spectra obtained in $NBu_4BBu_4$ showed many SSB signals at 343 K, it can be considered that there are no overall motion in the crystal. In the case of $^{1}$H MAS NMR spectra, the line-shapes were drastically changed at around $T_{tr2}$. These results of $^{1}$H and $^{13}$C NMR spectra indicate that motions detected in Phase II reduce $^{1}$H-$^{1}$H dipole-

dipole interactions and retain $^{13}C$ CSA. To satisfy these facts, we can introduce a model in which the alkyl chains of the $NBu_4^+$ and $BBu_4^-$ ions are rotated about C-C bonds rather than both ions performing overall motions. In the case of $NPen_4BBu_4$ crystals, the similar $^1H$ and $^{13}C$ MAS NMR spectra to those of $NBu_4BBu_4$ were obtained, therefore, it can be considered that there are similar motions of $NPen_4^+$ and $BBu_4^-$ ions to those observed in $NBu_4BBu_4$. In the case of $NBu_4BBu_4$ and $NPen_4BBu_4$ crystals, small $\Delta S_{tr1}$ values of 10.5 and 9.0 J $K^{-1}$ $mol^{-1}$ were observed, respectively, therefore it can be assumed that both ions perform no overall motions in Phase I of both salts.

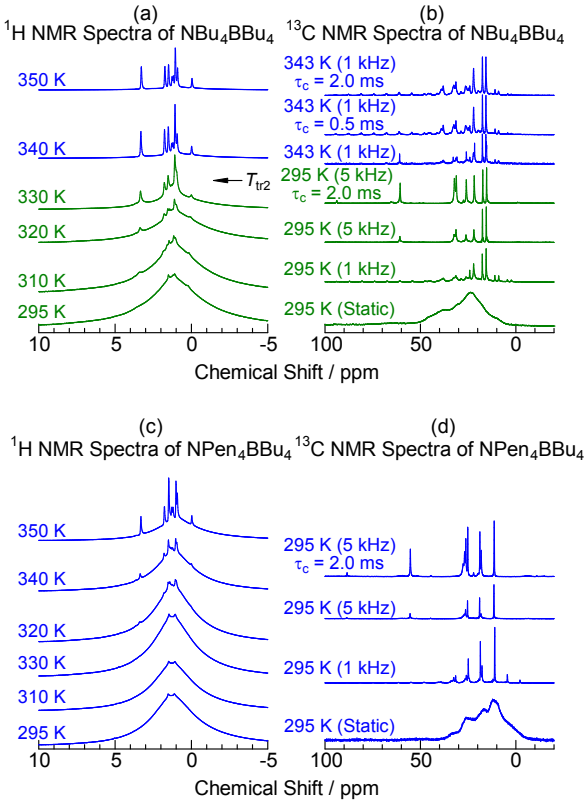


**Fig. 5. $^1$H MAS and $^{13}$C NMR spectra of $NBu_4BBu_4$ and $NPen_4BBu_4$. In this figure, spectra recorded in Phase II and III are shown by blue and green lines, respectively. (a), (c) $^1$H MAS NMR lines were observed at a MAS ratio of 10 kHz. (b), (d) $^{13}$C MAS NMR spectra measurements were performed at some MAS speeds (ratios are described in parenthesis). Contact times ($\tau_c$) are described on $^{13}$C CP/MAS NMR spectra**

## 3.4 Electrical Conductivity

Temperature dependences of electrical conductivities ($\sigma$) are plotted in Fig. 6. A function of log ($\sigma T$) shows the activation energy ($E_a$) of ionic diffusion by the following relationship:

$$\log(\sigma T) \propto -\frac{E_a}{RT} \tag{2}$$

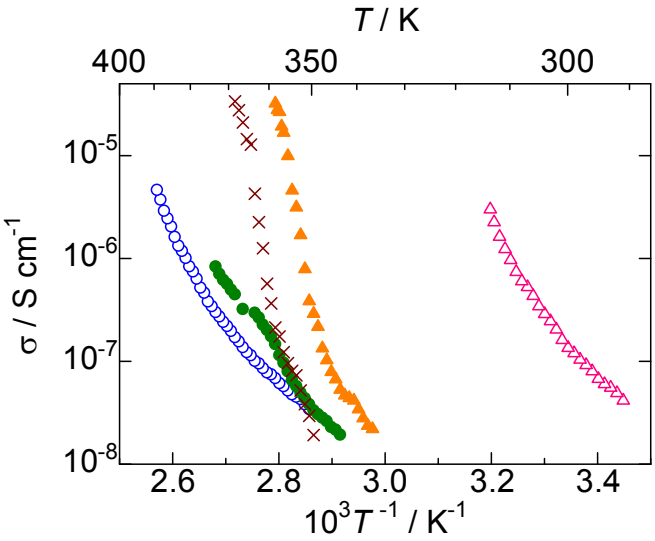


**Fig. 6. Electrical conductivity of $NMe_4BBu_4$(○), $NEt_4BBu_4$(●), $NPr_4BBu_4$(▫), $NBu_4BBu_4$(▲), and $NPen_4BBu_4$(×) as a function of temperature**

Plotting log ($\sigma T$) as a function of $T^{-1}$, the slope gives activation energies. The obtained $E_a$ values are summarized in Table 3. The activation energies estimated in $NMe_4BBu_4$, $NEt_4BBu_4$, and $NPr_4BBu_4$ are similar to those reported in ionic plastic crystals of $NR_4BEt_3Me$ (R = Me, Et) [30], although these $BBu_4$ salts form no plastic phases. Based on these results, it can be considered that the weak interaction among ions contributes to $E_a$ values for ionic translation motion: diffusion mechanisms of the new region of ionic plastic crystal is analogous to those of molecular plastic crystal, rather than those observed in ionic plastic crystals. Here, overall motions with large amplitudes (tumbling) can perform the resemble effect as isotropic reorientation i.e. preventing insertion of the counter ions into themselves. In contrast, large $E_a$ values were observed in $NBu_4BBu_4$ and $NPen_4BBu_4$ crystals. This can be explained by collision among long alkyl chains of the cation and the anion, because our NMR measurements showed that these salts have no overall motions in the crystals.

**Table 3. Activation energies in kJ $mol^{-1}$ obtained by electrical conductivity measurements**

| Compounds | |
|---|---|
| $NMe_4BBu_4$ | 60±10 |
| $NEt_4BBu_4$ | 60±5 |
| $NPr_4BBu_4$ | 60±20 |
| $NBu_4BBu_4$ | 150±20 |
| $NPen_4BBu_4$ | 195±10 |

## 4. CONCLUSION

This study showed the following results:

(i) The $NMe_4^+$ ion performs tumbling motion while the $BBu_4^-$ ion is restricted in the $NMe_4BBu_4$ crystal.

(ii) The $NEt_4BBu_4$ crystal has a small $\Delta S_{mp}$ value of 29.1 J $K^{-1}$ $mol^{-1}$ and large total entropy changes in solid phases (53.5 J $K^{-1}$ $mol^{-1}$). Large-amplitude overall motions (tumbling) of the ions were detected in Phase I, although it is classified as nonplastic-crystal.
(iii) The partial ions in the $NPr_4BBu_4$ crystal perform isotropic reorientation.
(iv) No overall motions were detected in the $NBu_4BBu_4$and $NPen_4BBu_4$crystals.
(v) Comparable $E_a$ values of ionic transfer were obtained in $\sigma$ measurements of the $NR_4BBu_4$ (R = Me, Et, Pr) crystals with those of ionic plastic crystals [30] although these salts have no plastic phases.

This study could not show isotropic reorientation of both cation and anion, however, it could be revealed that $NR_4BBu_4$ (R = Me, Et, Pr) crystals have overall motions. In the case of$BEt_3Me$ salts, isotropic reorientation is detected in $NMe_4BEt_3Me$ and $NEt_4BEt_3Me$ [30]. Therefore it can be considered that collision among long alkyl chains of $BBu_4^-$ ions effects on overall motions of ions. In contrast, based on the result (v), it can be regarded that overall motions with large amplitudes (tumbling) can perform the resemble effect as isotropic reorientation for ion transfer i.e. preventing insertion of the counter ions into themselves.

## COMPETING INTERESTS

Authors have declared that no competing interests exist.

## REFERENCES


1. Timmermans J. Plastic crystals: A historical review. J Phys Chem Solids.1961;18(1):1-8.
2. Solonin Yu M, Gorban VF, Graivoronskaya EA. Preparation of monocrystals of fullerite C60, crystal structure and determination of mechanical characteristics by microindentation method. Dopovidi Natsional'noi Akademii Nauk Ukraini. 2008;(4):114-119.Russian.
3. David WIF. Structural studies of C60 using high resolution neutron powder diffraction.Applied Radiation and Isotopes.1995;46(6/7):519-524.
4. Jin Y, Xenopoulos A, Cheng J, Chen W, Wunderlich B, Diack M, Jin C, Hettich RL, Compton RN, GuiochonG. Thermodynamic characterization of the plastic crystal and non-plastic crystal phases of $C_{70}$.Molecular Crystals and Liquid Crystals Science and Technology, Section A. 1994;257:235-250.
5. Takeda S, Atake T. Molecular motion and phase transition in the new substance $C_{60}$ fullerene. Plastic crystal $C_{60}$. Kotai Butsuri. 1993;28(3):183-190. Japanese.
6. Burns G, Dacol FH, Welber B. Lattice vibrational study of the phase transition in the plastic crystal adamantane (C10H16).Solid State Commun.1979;32(2):151-155.
7. Debeau M, Depondt P. Raman light scattering experiments of orientationally disordered crystals and the rigid molecule hypothesis. Journal of Chemical Physics and Physical Chemistry Organic. 1985;82(2-3):233-238.
8. Ganguly S, Fernandes JR, Rao CNR. Calorimetric, infrared and ESR studies of the plastically crystalline state of organic compounds. Advances in Molecular Relaxation and Interaction Processes. 1981;20(3):149-163.
9. Kobashi K, Etters RD. Theory of diffuse x-ray scattering due to orientational correlation in plastic molecular crystals. Molecular Phys.1982;46(5):1077-1083.
10. Moriya K, Matsuo T,Suga H. Thermodynamic properties of alkali and thallium nitrites: The ionic plastically crystalline state. Thermochim Acta.1988;132:133-140.

11. Moriya K, Matsuo T, Suga H. Calorimetric and dielectric studies of phase transitions in rubidium nitrite. Bull Chem Soc Jpn. 1988;61(6):1911-1916.
12. Moriya K, Matsuo T, Suga H. Phase transition and freezing of disordered ionic orientation in cesium nitrite crystal. Chem Phys Lett. 1981;82(3):581-585.
13. Moriya K, Matsuo T, Suga H, Seki S. Calorimetric and dielectric studies of phase transition in thallium(I) nitrite crystal. Chem Lett.1977;12:1427-1430.
14. Moriya K, Matsuo T, Suga H. Phase transition and freezing of ionic disorder in cesium and thallium nitrite crystals. J Phys Chem Solids.1983;44(12):1103-1119.
15. Furukawa Y, Kiriyama H. Magnetic relaxation of thallium nuclei and ionic motion in solid thallium(I) nitrite. Chem Phys Lett. 1982;93(6):617-620.
16. Furukawa Y, Nagase H, Ikeda R, Nakamura D. Cationic self-diffusion in ionic plastic phases of thallium nitrite and nitrate and in thallium thiocyanate. Bull Chem Soc Jpn. 1991;64(10):3105-3108.
17. Kenmotsu M, Honda H, Ohki H, Ikeda R, Erata T, Tasaki A, Furukawa Y. Ionic dynamics in plastic crystal $KNO_2$ studied by $^{39}K$ and $^{15}N$ NMR.Z Naturforsch A.1994;49(1-2):247-252.
18. Honda H, Kenmotsu M, Ohki H, Ikeda R, Furukawa Y.Dynamics of nitrite ions in ionic plastic crystal $RbNO_2$ studied by nitrogen and rubidium NMR. Ber Bunsenges Phys Chem.1995;99(8):1009-1014.
19. Honda H, Ishimaru S, Onoda-Yamamuro N, Ikeda R. Dynamics of nitrite ions in the ionic plastic crystal $TlNO_2$ studied by $^{15}N$ and $^{205}Tl$ NMR. Z Naturforsch A.1995;50(9):871-875.
20. Honda H, Kenmotsu M, Onoda-Yamamuro N, Ohki H, Ishimaru S, Ikeda R, Furukawa Y. $^{15}N$ and $^{133}Cs$ solid NMR studies on ionic dynamics in plastic $CsNO_2$. Z Naturforsch A. 1996;51(5/6):761-768.
21. Honda H, Onoda-Yamamuro N, Ishimaru S, Ikeda R, Yamamuro O, Matsuo T.Dielectric study on ionic orientational disorder in the low-temperature phases of ionic plastic crystal $KNO_2$. Ber Bunsenges PhysChem.1998;102(2):148-151.
22. Onoda-Yamamuro N, Honda H, Ikeda R, Yamamuro O, Matsuo T, Oikawa K, Izumi F.Neutron powder diffraction study of the low-temperature phases of $KNO_2$. J Phys Condens Matter.1988;10(15):3341-3351.
23. Honda H. Ionic dynamics in the ionic plastic crystal $NH_4NO_2$.Z Naturforsch A. 2007;62(10/11):633-638.
24. Ikeda R. Dynamic behavior of molecular ions in new mesophases between solid and liquid. Recent Res Devel Chem Physics.2004;5(2):257-301.
25. Adebahr J, Grimsley M, Rocher N M, MacFarlane DR, Forsyth M. Rotational and translational mobility of a highly plastic salt: Dimethyl pyrrolidinium thiocyanate. Solid State Ionics.2008;178(35-36):1793-1803.
26. Seeber AJ, Forsyth M, Forsyth CM, Forsyth SA, Annat G, MacFarlane DR. Conductivity, NMR and crystallographic study of N,N,N,N-tetramethylammonium dicyanamide plastic crystal phases: An archetypal ambient temperature plastic electrolyte material. Phys Chem.2003;5(12):2692-2698.
27. Ono H, Ishimaru S, Ikeda R, Ishida H. Ionic plastic phase in piperidinium hexafluorophosphate studied by solid NMR, x-ray diffraction, and thermal measurements. Ber Bunsenges Phys Chem.1998;102(4):650-655.
28. Ono H, Ishimaru S, Ikeda R, Ishida H.$^{1}H$, $^{2}H$, $^{19}F$, $^{31}P$ and $^{35}Cl$ NMR Studies on Molecular Motions in Ionic Plastic Phases of Pyrrolidinium Perchlorate and Hexafluorophosphate. Bull Chem Soc Jpn. 1999;72(9):2049-2054.
29. Honda H, Ishimaru S, Ikeda R.Ionic dynamics in $LiNO_2$ studied by $^{7}Li$ and $^{15}N$ solid NMR. Z Naturforsch A.1999;54(8/9):519-523.

30. Hayasaki T, Hirakawa S, Honda H.New ionic plastic crystals of $NR_4BEt_3Me$ (R = Me and Et) and $NR_xR'_{4-x}BEt_3Me$ (R = Et, R' = Me and Pr, x = 1-3) in a new class of plastic crystals. Bull Chem Soc Jpn. 2013;86(8):993-1001.
31. Kabatc J, Paczkowski J. The photophysical and photochemical properties of the oxacarbocyanine and thiacarbocyanine dyes. Dyes and Pigments.2004;61(1):1-16.
32. Frisch MJ, Trucks GW, Schlegel HB, Scuseria GE, Robb MA, Cheeseman JR, Montgomery JA Jr., Vreven T, Kudin KN, Burant JC, Millam JM, Iyengar SS, Tomasi J, Barone V, Mennucci B, Cossi M, Scalmani G, Rega N, Petersson GA, Nakatsuji H, Hada M, Ehara M, Toyota K, Fukuda R, Hasegawa J, Ishida M, Nakajima T, Honda Y, Kitao O, Nakai H, Klene M, Li X, Knox JE, Hratchian HP, Cross JB, Adamo C, Jaramillo J, Gomperts R, Stratmann RE, Yazyev O, Austin AJ, Cammi R, Pomelli C, Ochterski JW, Ayala PY, Morokuma K, Voth GA, Salvador P, Dannenberg JJ, Zakrzewski VG, Dapprich S, Daniels AD, Strain MC, Farkas O, Malick DK, Rabuck AD, Raghavachari K, Foresman JB, Ortiz JV, Cui Q, Baboul AG, Clifford S, Cioslowski J, Stefanov BB, Liu G, Liashenko A, Piskorz P, Komaromi I, Martin RL, Fox DJ, Keith T, Al-Laham MA, Peng CY, Nanayakkara A, Challacombe M, Gill PMW, Johnson B, Chen W, Wong MW, Gonzalez C, Pople JA. Gaussian 03, Revision B.04: Gaussian Inc: Pittsburgh PA; 2003.
33. Saito H, Tuzi S, Tanio M, Naito A. Dynamic aspects of membrane proteins and membrane-associated peptides as revealed by $^{13}C$ NMR: lessons from bacteriorhodopsin as an intact protein. Annu Rep NMR Spectro. 2002;47:39-108.
34. Gerstein BC, Dybowski CR. Transient Techniques in NMR of Solids. Academic Press: New York; 1985.



*Peer-review history:*
*The peer review history for this paper can be accessed here:*
*http://www.sciencedomain.org/review-history.php?iid=528&id=16&aid=4697*